24th COBEM - 2017

24th ABCM International Congress of Mechanical Engineering
December 3-8, 2017, Curitiba, PR, Brazil

COBEM-2017-0724
COATING WELDIGN WITH CORED WIRE AND MONITORING WITH ACCELEROMETER

Marcos Vinícius Tavares da Silva
Émillyn Ferreira Trevisani Olivio
Federal Techonological University of Paraná, Cornélio Procópio, PR, CEP 86300-000, Brazil
marcosvinicius.mvt@gmail.com
emillynf@utfpr.edu.br
Celso Alves Correa
Federal Techonological University of Paraná, Cornélio Procópio, PR, CEP 86300-000, Brazil
cacorrea@utfpr.edu.br

Abstract. *The welding coating was applied by the tubular wire process shielding gas in the flat position with a conventional current. The base metal used SAE 1020 and the addition of metal used was stainless stell martensitic 410 (CA6MN). Were made assay by varying the welding parameters such as average current, the distance part contact tip and welding speed. Collected data of current, voltage and acceleration with the aid of an accelerometer, these data were analyzed using MatLab software. In the most current level we obtained the best morphology of the weld bead. Through the current graphics, voltage and acceleration was possible to determine the stability of the electric arc during welding.*

Keywords: *coating welding, vibration, acceleration.*

1. INTRODUCTION

Coating welding with tubular wire is widely used for parts recovery or base metal improvement, has the same welding application parameters that can be measured and analyzed determine the quality of the coating applied. By mean of voltage, acceleration and vibration graphs it is possible identification when one drop detaches from the electrode and collides with the base metal. The present text aims to show the results of the application of martensitic stainless steel coating 410 (CA6MN) in SAE 1020 steel under certain welding conditions.

2. METHODOLOGY

2.1 Experimental

In the execution of the project, the steel SAE 1020 was used as base metal with the fallowing dimensions: 185.00 mm long, 63.50 mm wide and 12.70 mm thick, the chemical specifications are found in Table 1.

Table 1. Chemical composition SAE 1020 steel

Elements	C	Mn	Si	P	S	Cu	Cr	Ni	Sn	N (ppm)
content in %	0,18/ 0,23	0,30/ 0,60	0,10/ 0,30	0,030 máx.	0,035 max.	0,200 max.	0,150 max.	0,150 max.	0,060 max.	80
tensile strength (Kgf/mm²)				45	yield streength (kgf/mm²)					25

The addition metal used a martensitic stainless steel tubular wire 1.2 millimeters in diameter, specified as AWS EC410NiMo MC, the chemical specifications of the addition steel are found in Table 2.

Table 2: Chemical composition EC410NiMo

Elements	C	Si	Mn	P	S	Cr	Ni	Mo
content in %	0,027	0,44	0,59	0,024	0,006	12,5	4,86	0,43
tensile strength (MPa)			910	yield streength (MPa)				830

In order for all specimens to be welded in the same manner, a welding tortoise was used and the listed equipment were used:

- Multiprocessing welding source with the following specifications: universal model 450, direct or alternating current, input voltage 220, 380 or 440 V three-phase.
- Water cooled straight torch with the following specifications: MIG straight torch TBI 511 Aut – 2.0M, usable diameter 1,2mm to 2,4mm.
- Power car: welding tortoise with controllable displacement of X and Y axes.
- Current transducer for acquisition board: model 600R010VAC-220VAC, measuring range -600 to 600A for direct current.
- Voltage transducer for acquisition board: model 100V010VAC-220VAC, measuring range 0 to 110V for direct current.
- Industrial accelerometer: model KS80D with frequency 0,13 to 22.000 Hz

2.2 Experimental methodology

Before starting the tubular wire coating process, a procedure was performed with the test body to obtain a grease, oil and contaminant free surface. In order to obtain this surface, the test bodies were sandblasting with G-25 S-280 angular steel shot with degree of hardness D.

After the blasting procedure, the specimen was heated in an NT-280 mufle furnace at a temperature of 200ºC. After reaching this temperature, they were taken to fiction and the welding process started when the temperature reached 150ºC. This procedure was performed to have an intercept temperature of 150º C.

In process de temperature of the sample is higher than the temperature allowed by the accelerometer, so is was placed laterally on the table and in the center of the test body so that it did not suffer damages with the temperature of the piece.

For the accomplishment of the experiments some parameters were defined like constant. This parameters were defined according to the bibliography and later were left to be confirmed. In addition to these constant parameters, for the experiment other parameters were adopted as varied, they are: average current, welding speed, distance of the contact nozzle of the piece. Four different experiments were performed, which are found in the table below:

Table 3: Variation of parameters used in welding.

Amperes (A)	Welding speed (mm/min)	Distance piece nozzle (DPN)	Hz	Test
200	300	36	-	1
200	350	30	-	2
230	300	36	-	3
230	350	30	-	4

3. RESULTS AND DISCUSSION

The results were divided into two parts. The first presents a morphology of the weld beads generated for each test performed. The second part presents the generated graphs with the help of MatLab software. The graphs were used as, current x time, voltage x time and acceleration x time. Later, the fast Fourier transform was applied to analyze the graphs in the frequency domain. After this treatment, graphs of acceleration x frequency were generated.

2.3 **Morphology of cords**

In the welding coating, it is important that the weld bead is as wide as possible and that the penetration of the weld is not so great. For analysis of this study the following parameters were analyzed: width (L), reinforcement (R), penetration (P), as exemplified in figure 1.

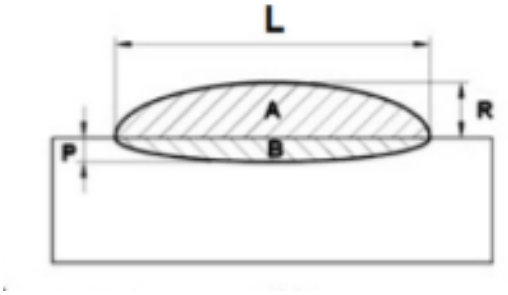

Figure 1. Weld cord parameters

After defining the welding parameters and with the results found, a table was set up showing the comparison between the four types of experiments performed. These results are show in table 4.

Table 4: Weld bead morphology table for 200 A and 230 A

Amperes (A)	Welding speed of 300 (mm/min)	Welding speed of 350 (mm/min)
200 A	 DPN – 36 mm	 DPN – 30 mm
230 A	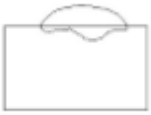 DPN – 36 mm	DPN – 30 mm

After obtaining the morphology of the weld bead, the parameters such as width, reinforcement and penetration were measured. The values found are show in table 5.

Table 5: Weld bead parameters

Amperes (A)	Welding speed (mm/min)	DPN (mm)	width (mm)	reiforcement (mm)	penetration (mm)
200	300	36	9,00	4,2	2,49
200	350	30	8,48	3,98	1,86
230	300	36	13,51	3,29	2,00
230	350	30	10,54	3,19	1,94

Analyzing the morphology of the weld bead and the parameters found it is possible to make some observations. By increasing the welding speed using both the 200 A current and the 230 A current the width obtained in the two weld beads decreased, in which case the variation of the penetration and the reinforcement were small.

A very noticeable difference when analyzing the two tables presented is the relation for the increase of welding current. When the current is increased from 200 A to 230 A, the width obtained in the weld bead when coating is made becomes better.

3.1. Results of signal acquisition

The collected date of current, voltage and acceleration were worked in the software Matlab and plotted in graphs for analysis, the graphs were generated as current by time, voltage by time and acceleration by time. The data were worked over a time interval of 20s to 30s.

The order of the experiments presented in table 3 was defined as the same order in the presentation of the results generated in Matlab, and the results are show in figure 2.

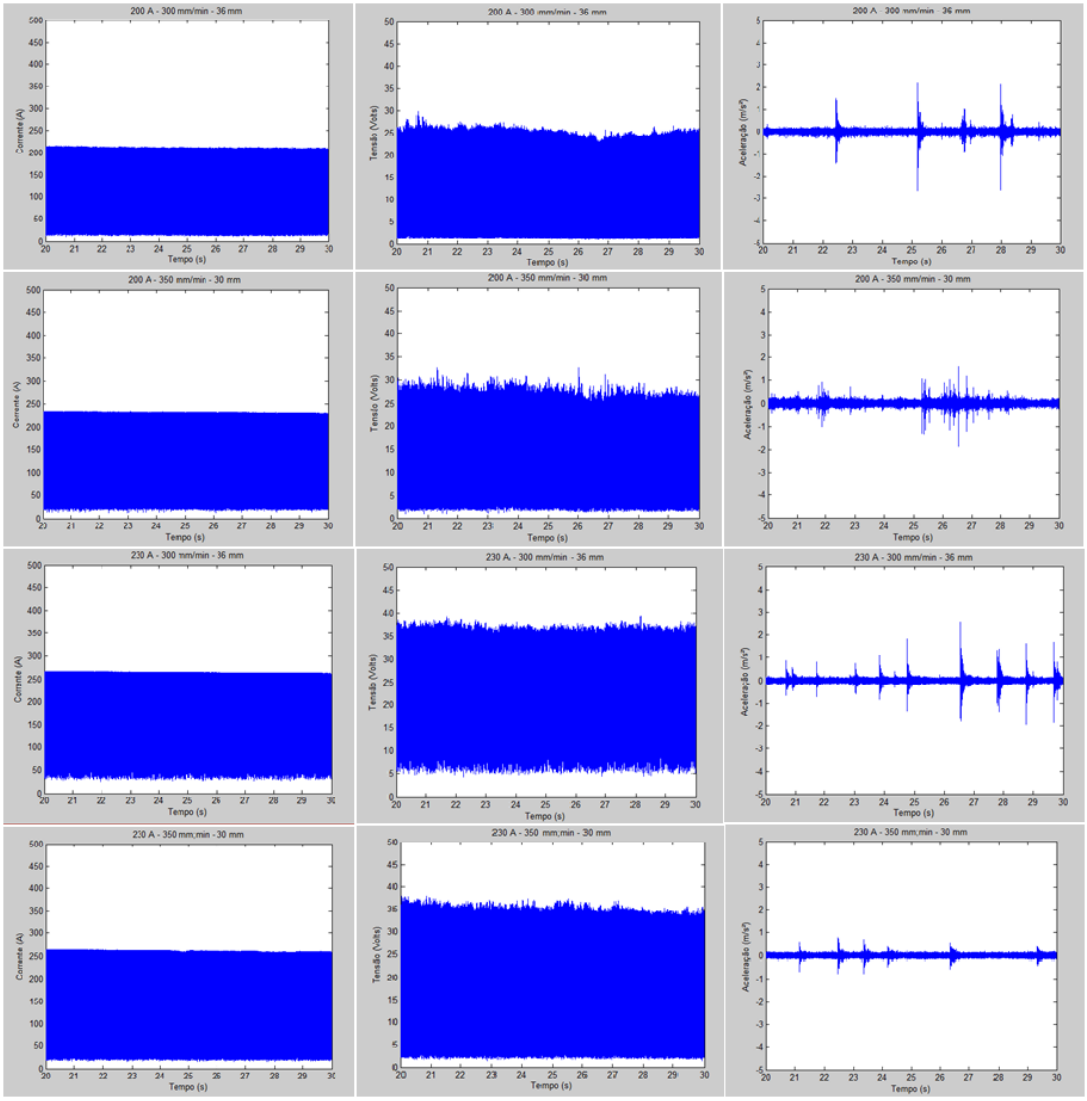

Figure 2. Graphs of current x time, voltage x time, acceleration x time

In addition to the results plotted in the graphs, their respective values RMS, current, voltage and acceleration, were obtained for each graph previously demonstrated and were grouped in table to facilitate the purchase, table 6 demonstrates these results.

When analyzing the acceleration data obtained from RMS and compare with the graphs previously demonstrated, figure two, can notice that the values represent well the behavior of the graphs. The experiment 4 has the lowest instability, the highest peak found in the time band has a maximum acceleration value close to 1 m/s² and the RMS value is 0.05820 m/s².

Comparing RMS values of current and voltage obtained with the values presented in the graphs, it can be noted that there is an approximation between them and that the comparison between the four experiments regarding these values is not feasible. On the other hand, the values of acceleration present great possibilities of analysis. Due to this possibility, the RMS values for acceleration were compared in bar graph form, show in figure 3. In the graphs the values are represented following the order of the experiments.

Table 6: Current (RMS), voltage (RMS) and acceleration (RMS) data for the time-generated graphs from 20s to 30s.

Amperes (A)	welding speed (mm/min)	DPN (mm)	current RMS (A)	voltage RMS (V)	acceleration RMS (m/s^2)
200	300	36	166,0988	20,1648	0,115
200	350	30	182,5528	22,1737	0,0813
230	300	36	213,2463	30,3707	0,0975
230	350	30	204,2958	27,8079	0,0582

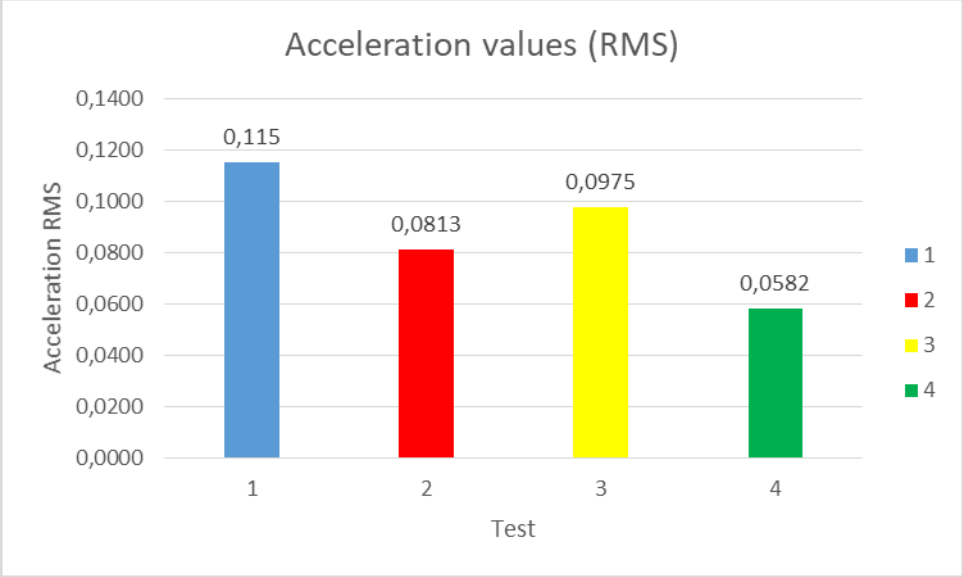

Figure 3. Bar graph with value RMS of acceleration.

The data analysis was also done the frequency domain so that a better detail of the obtained data can be obtained. In order to analysis the data in these domain, it was necessary to use the Fast Fourier Transform programmatically using MATLAB software.

The acceleration graphs were plotted for the four experiments performed and the value used for the abscissa coordinate was 500 Hz. This value was defined based on the network value of 60 Hz. Figure 4 shown the acceleration graphs with the welding current of 200 A, welding speed of 300 mm/min and DPN 36 mm, in the second graph with the welding current of 200 A, welding speed of 350 mm/min and DPN 30 mm, for test 1 and 2 respectively.

In the figure 5 it is showing the acceleration graphs with the welding current of 230 A, welding speed current of 300 mm/min and DPN 36 mm, in the second graph with the welding current of 200 A, welding speed of 350 mm/min and DPN 30 mm., for test 3 and 4 respectively.

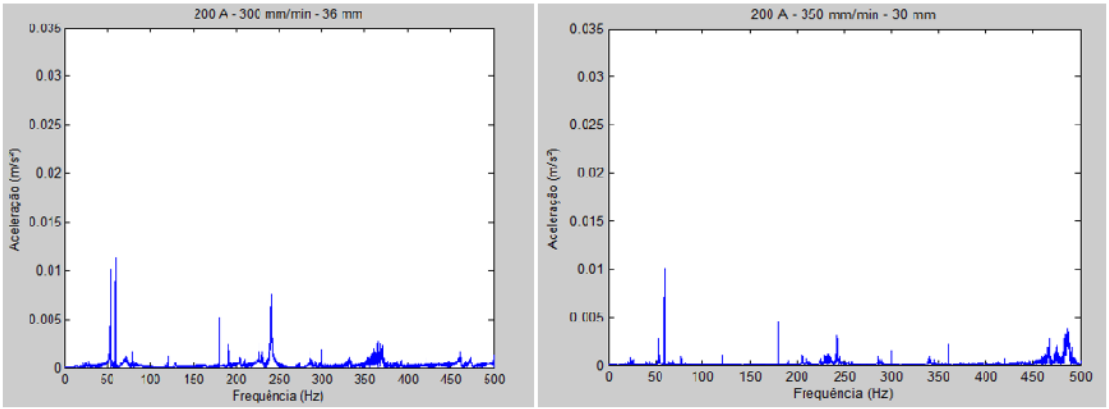

Figure 4. Graph of acceleration x frequency for current of 200 A, test 1 and test 2 respectively.

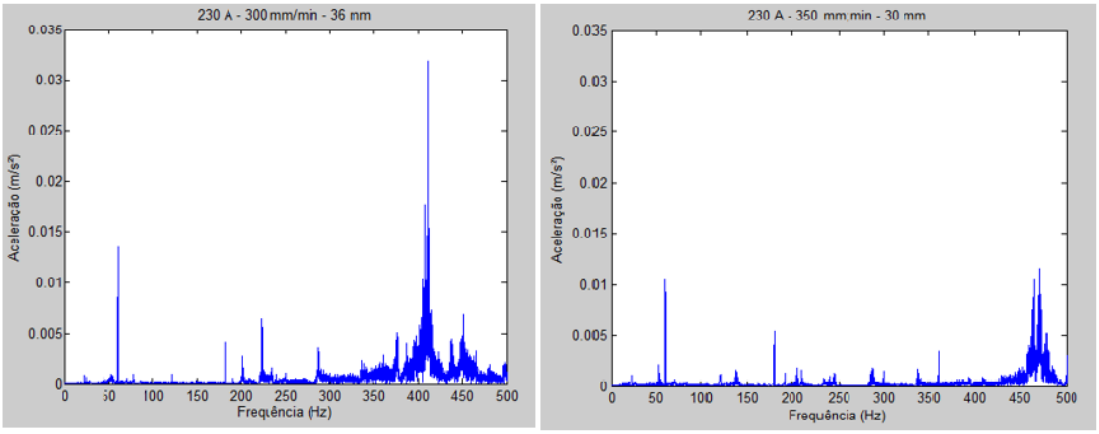

Figure 5. Graph of acceleration x frequency for current of 230 A, test 3 and test 4 respectively.

Be analyzing the graphs show, we can note that the first peak was generated at a frequency of 60 Hz. This peak was generated due to the moment the shock of the metal drop form the electrode to the base metal occurs. This shock generates a vibration that is picked up by the accelerometer. ARATA (1981) reported this event by using an accelerometer in welding.

It is possible to notice that for the graphs that present a higher welding speed and a smaller distance from the contact nip of the part, they presented smaller amounts of peaks. That is, for current of 200 A, test 2 presents the least amount of peaks and for the current of 230 A, test 4 presents the smallest number of peaks. We can see that in the graph of figure 5 for test 3, the peak values reached by the peaks are higher than the peak values reached by the peaks of test 4. This shows that in test 3 we had more vibration of the base metal

According to ARATA (1981) the peaks will appear cyclically in the acceleration graph, due to the continuous transfer of the electrode to the base metal. When analyzing the graphs we can see that there are peaks that appear outside the 60 Hz cycle. These peaks can be explained due to spatter occurring in the material during the welding process, knowing that these spatter also cause the base metal to vibrate, we can define that the smaller the number of peaks out of the cycle the smaller the amount of spattering.

4. CONCLUSION

By means of the results obtained by analyzing the generated graphs and by the morphology of the coating cords, it was possible to analyze how each parameter interfered in the weld bead. As well an amount of vibration generated by droplets of addition metal that collide with the base metal.

It was possible to analyze the variation and the repetition of the peaks found in the generated graphs, which show a cyclic deposition of addition material.

When analyzing the morphology of the weld bead, we can see that the strings that presented the best values were those made using the current of 230 A and consequently the best results in the acceleration graphs were obtained using the same current value, we can find in the peaks that repeat cyclically with fixed values of frequency. These low acceleration values in the acceleration frequency plot demonstrate that little vibration occurred in the melt pool.

5. REFERENCES

ARATA, Yoshiaki; et al. Investigation on Welding Arc Sound: Vibration Analysis of Base Metal during Welding. Osaka University Knowledge Archive: 1981.

RAO, S., Mechanical Vibrations. São Paulo: Pearson Education do Brasil. 2009

SUYAMA, Daniel Iwao. A contribution to the study of internal turning in hardened steels c1. 2014. 136 f. PhD Thesis in Mechanical Engineering - State University of Campinas, Campinas. 2014

WANG. W., LIU, S. and JONES, J.E. 1995 Flux Cored Arc Welding: Arc Signals, Processing and metal Transfer Characterization, Welding Journal 74(11): 369s377s.

6. RESPONSIBILITY NOTICE

The authors are the only responsible for the printed material included in this paper.